Scientia Iranica (2025) **32**(1): 6574

Sharif University of Technology

Scientia Iranica

Transactions on Computer Science & Engineering and Electrical Engineering

https://scientiairanica.sharif.edu

Statistical analysis based load frequency control of multi-area system with nonlinearities using 2-DOF-PID controller with application of improved sine-cosine algorithm optimizer

Neelesh Kumar Gupta*, Manoj Kumar Kar, Arun Kumar Singh

Department of Electrical Engineering, NIT Jamshedpur, Jamshedpur, India-831014.

* Corresponding author: 2018rsee008@nitjsr.ac.in (N. Kumar Gupta)

Received 4 March 2022; received in revised form 31 January 2023; accepted 17 July 2023

Keywords

Improved sine-cosine algorithm;

Statistical analysis;

Load Frequency Control (LFC);

WSRT;

FOPID;

2-DOF-PID.

Abstract

In this article, for Load Frequency Control (LFC) in power system an improved sine-cosine algorithm is proposed with 2-DOF-PID controller. To facilitate the inspection, a multi-area test system (three area) has been developed. Additionally, several physical restrictions have been taken into account while investigating practical power system analysis. For every scenario considered for the experiment, the suggested approach has been employed as the optimizer of parameter of the controller of LFC. 2-DOF-PID controllers has the ability to quickly reject disturbances without noticeably increasing overshoot in set point tracking, have been utilised as the controller of LFC. The PIDF and FOPID controllers has been compare with 2-DOF-PID controller to evaluate the usefulness of it. The simulation results of SCA, SSA, ALO, and PSO are some of the algorithms with which of the proposed modified algorithm were compared, in three distinct scenarios: disturbance in three areas, disturbance in two areas, and the final scenario with physical restrictions. Wilcoxon Sign Rank Test (WSRT) has been use for the statistical analysis and 20 separate times was carried out in order to further prove the supremacy of the suggested strategy.

1. Introduction

The primary goal of the contemporary power system is to deliver a consistent and dependable power supply. This is possible when the balance between power demand and generation is preserved. One crucial factor that helps determine the balance between supply or generation and demand is frequency. The relationship between frequency and load is negatively correlated. Therefore, if frequency is more than its scheduled value, it means that the load is less than the generation, and if it is lower than its actual value, it means that the load is greater on the system than the supply. It is crucial to keep the frequency at its set value, which may be done using a method called Load Frequency Control (LFC) [1]. LFC is primarily in charge of keeping frequency drift within allowable bounds. Additionally, it keeps the tie-line power drift across multi-area systems at a tolerable level. The mechanical input to the power generator is used to balance the supply and demand for energy, and the LFC regulates this input in accordance with the demands. The LFC essentially does the following:

- Minimize the transient response and time error, as well as Nullify the steady state frequency error resulting by a step load fluctuation;
- Provides the emergency requirement of power in any region by the other areas;
- Eliminated the immobile variation in tie-line power due to step load retribution to zero.

A details study of the LFC for the conventional system is given in the [2]. Various type of power system like single area system, two area system with thermal system, two area with thermal hydro, and three area system has been discussed. Also, different control strategies like classical control approaches, optimal control approaches, adaptive and self-tuning approaches has been discussed by the author but all these approaches have some drawback which leads to soft computing techniques based approach. A PSO based controller is designed by Shayeghi for the LFC of a the three area system in [3]. The design of PID controllers with various tuning method for LFC in past, present, and its challenges is discusses by Hote and Jain [4].

To cite this article:

N. Kumar Gupta, M. Kumar Kar, A. Kumar Singh "Statistical analysis based load frequency control of multi-area system with nonlinearities using 2-DOF-PID controller with application of improved sine-cosine algorithm optimizer", *Scientia Iranica* (2025) **32**(1): 6574

https://doi.org/10.24200/sci.2023.60059.6574

In [5] a PID controller designed using PSO for the two area system has been discussed. Gravitational search Algorithm based PID controller has been suggested by R. sahu for a two area thermal system having nonlinearity of GRC for both turbine and compression of the various performance index ITAE, ITSE, ISE, IAE has been show in which ITAE give better performance [6]. ALO base PI controller has been suggested in [7] for the interconnected three area power system where a compression is shown between ALO, PSO and genetic algorithm in which ALO perform better for this system. A fuzzy based controller has been discuss for the two area power system with and without GRC in [8]. Sahu et al. suggested 2-DOF-PID controller for a two area system having GDB [9]. Latif et al. has reviews the history of the use of the fractional order controller for the LFC in [10]. It is found in [10] the various type of fractional type of the controller like FOI, FOPI, FOPID, FOPIDN, TID, FOPDPI etc. has been use by the researches but among then FOPID is most used fractional order controller. Taher et al. used FOPID controller based of imperislist competitive algorithm for the interconnected system and result are compare with PID controller outcome to prove its robustness [11]. Similarly, in [12-14] FOPID has been used for various type of power system and result of the of controller has been compare with some others controller where FOPID controller perform better. Jagatheesan has compare various type of objective function for different type of the power system [15]. Salp swarm based PID controller is designed for a hybrid power system and various objective function has been compare where ITAE is giving better result [16]. The slap swarm algorithm has been used in the [17-19] as the optimization techniques for the LFC controllers. The Ant-lion optimizer algorithm has been used in [20,21], as the LFC controller optimizer for different type of the power system in the resent time. In the resent time Sine cosine algorithm has been widely used in LFC for the controller parameter optimizer as shown in [22–25].

According to the literature review, the researchers who studied LFC mostly concentrated on three things: building a new controller, suggesting novel optimization strategies and modelling various varieties of power system. The SCA is a freshly established algorithm that has been used to address many technical problems. SCA, however, experiences delayed convergence and is prone to stalling in local optima. SCA is enhanced for increased performance, and the LFC controller's controller is tuned using the Improved SCA (ISCA) approach. The 2-DOF-PID controller controlled 3-area system having physical restrain has been planned and LFC implemented using ISCA. The objective function employed in this study is ITAE, and by minimising ITAE, several transient parameters have been improved.

The statistical analysis has been done to further establish the suggested method's superiority. Each technique has been performed 20 times in total for the statistical analysis. In this instance, the Wilcoxon Sign Rank Test (WSRT) employed to execute statistical analysis which is a sign test in which the signs +, -, and ≈ denote the superior, inferior, and equal with respect to the comparable one.

The following is a description of the proposed work's contributions:

- Three-area test systems are modelled and taken into account for case studies;
- The suggested method's superiority has been demonstrated by comparisons with the original SCA, ALO, SSA, and PSO utilising both unimodal and multimodal benchmark functions;
- Statistical analysis and WSRT is performed for each benchmark function with proposed method;
- The performance of three different controller types-PID, 2-DOF-PID, and FOPID-is assessed;
- The LFC controller variables are tuned using the suggested ISCA, and the effectiveness is then assessed against that of a few other recently established algorithms, including SCA, ALO, SSA, and PSO;
- In order to get at the conclusive conclusions, statistical analysis and WSRT are used for the first time in the research of LFC;
- Investigations have been done on the effect that physical limitations have on system performance.

The remaining sections of the article are organized as follows. In Section 2, the recommended power system is displayed. Section 3 gives details on the suggested controller. Section 4 provides more information on the suggested optimization method. In Section 5, the term ``problem formulation" is defined. Section 6 discusses the findings, and Section 7 provides a summary of the conclusions.

2. Proposed power system

It is possible to create a balance between production and demand of electric power by maintaing the frequency at its nominal value so that there should not be any drift in the frequency. Two control loops are used in LFC which are primary and secondary. Primary loop work locally and give fast response but can’t be able to bring back drift in frequency to zero. Hence, we required a secondary loops which will bring back frequency deviation to zero The LFC of a three-area interconnected thermal power system is taken into consideration and given in the current planned study. The three areas under consideration each have a thermal power system of identical size, and tie lines connect them all. The speed governor, turbine, power system (Generator), and speed regulator are the main components of the thermal power system.

The transfer function of speed governor component is given as $\left(\frac{1}{1+sT_g}\right)$The below equation show the input and output of speed governor which consisted of two input i.e., ΔP_{ref} and ΔF and one output $\Delta P_G(s)$.

$$\Delta P_G(s)=\left(\Delta P_{ref}(s)-\frac{\Delta F(s)}{R}\right)\left(\frac{1}{1+sT_g}\right).$$

The transfer function of turbine is given as:

$$G_T(s)=\frac{1}{1+sT_t}$$

and transfer function of the generator and load is given as:

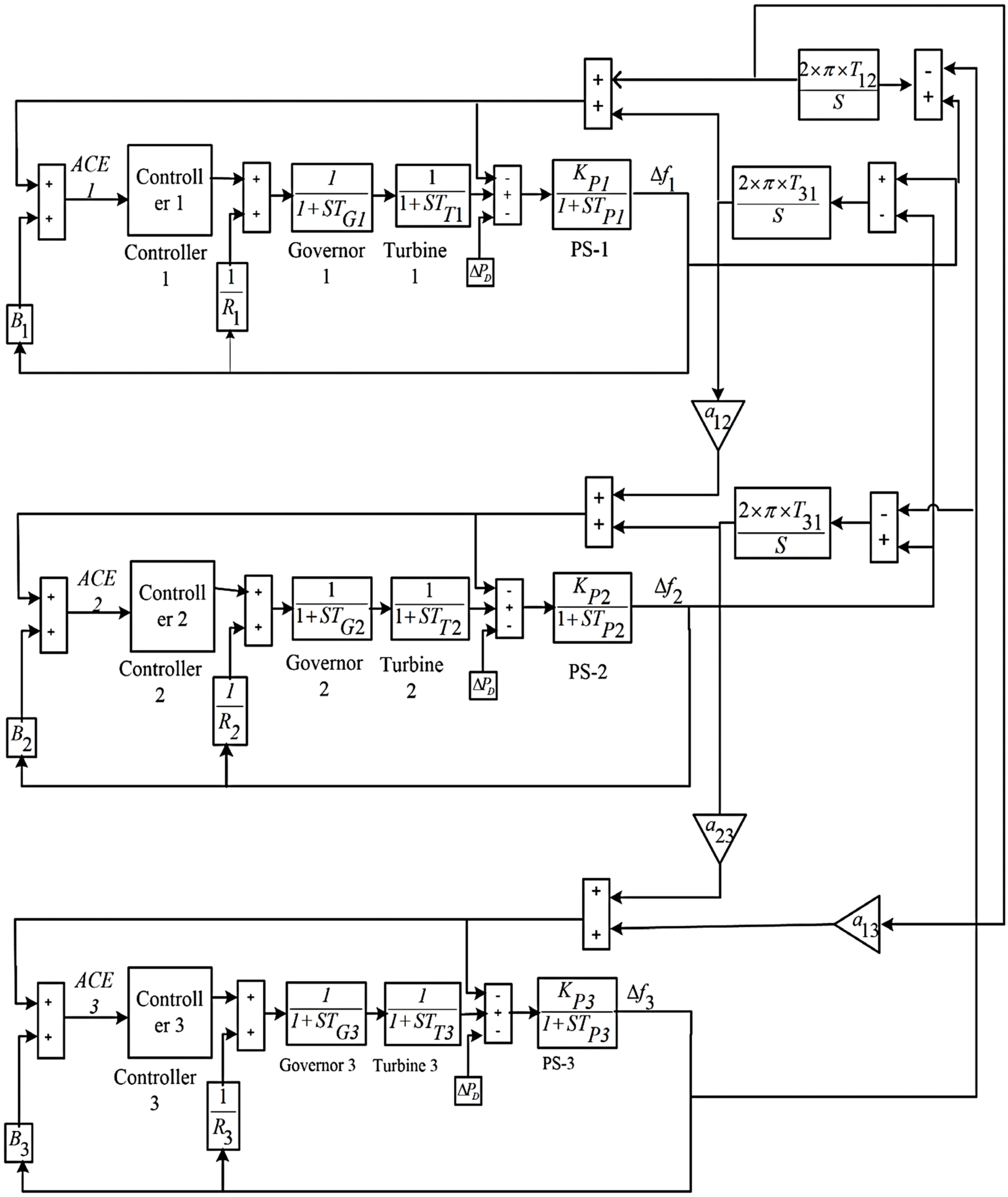

Figure 1. Block diagram layout of three area power system.

$$G_P(s) = \frac{K_P}{1+sT_P}.$$

In LFC each area will get three input and give two outputs. ΔP_{ref} load disturbance ΔP_D and ΔP_{tie} are the three inputs where ΔF and ACE (Area control error) are two outputs. ACE is given as:

$$ACE = B\Delta F + \Delta P_{tie},$$

where B is the frequency bias parameter.

Figure 1 depicts a transfer function model of a three-area interconnected power system and Appendix 1 lists the nominal values of the power system parameters as show in [9]. Each power generating unit manages its own load demand during nominal loading conditions and keeps the power system parameter within the allowed range. Performance of the system was impacted by time domain specification values (damping oscillation, significant peak over and under shoot with long settling time) during periods of swift load demand. The secondary controller must be properly designed and implemented in order to consistently provide high-quality power to all users.

3. The suggested controllers

Many different PID controller variations have been employed by the researcher for a long time, as shown by the literature review. The main reason for this is that it is straightforward and capable of producing outcomes that

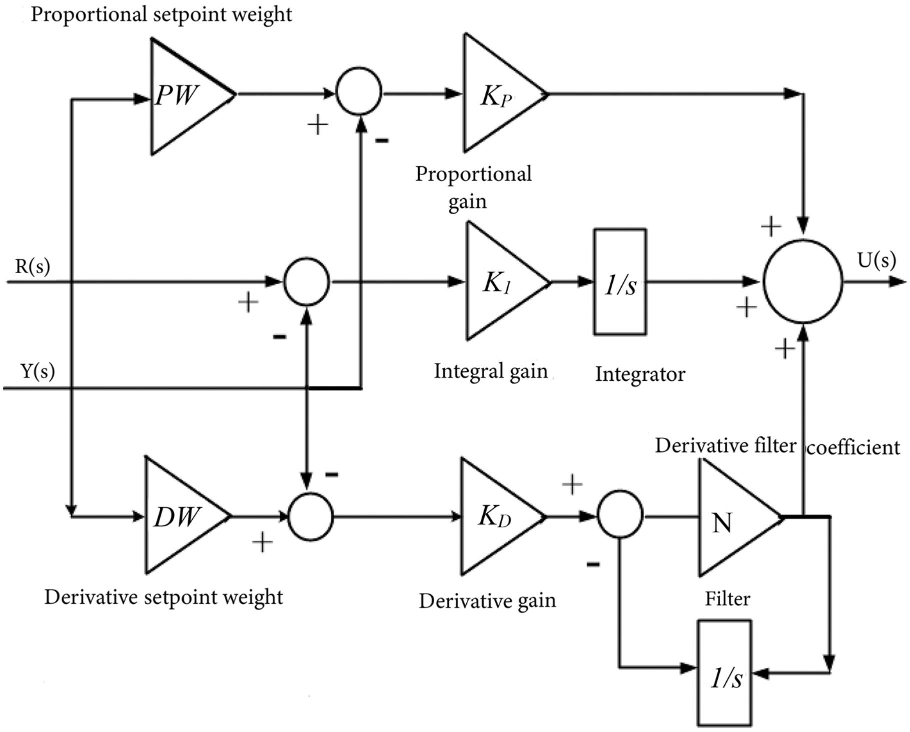

Figure 2. Block diagram layout of 2-DOF-PID controller.

can be relied upon. Due to its capacity to quickly reject disturbances without significantly increasing overshoot in set point tracking, the 2-DOF-PID controller, a very powerful variant of the PID controller, is considered as the LFC controller in this study [9,26]. The DOF, or degree of freedom, refers to how much of a closed loop transfer function may be handled in a control system with clarity. Figure 2 depicts the fundamental layout of this controller, which features two distinct loops. The controller is given two inputs, one of which is a reference and the other of which is the system's output. The controller uses the error signal created by the difference between these two signals to create the controller output signal, which is composed of proportional, integral, and derivate components according to weight. Eq. (1) illustrates the 2-DOF- PID's mathematical formulation.

$$U(s) = K_P\left(\left(PW\right)R(s) - Y(s)\right) + \frac{K_i}{s}\left(R(s) - Y(s)\right) + \frac{K_d s}{Ns+1}\left(\left(DW\right)R(s) - \mathrm{Y}(s)\right). \tag{1}$$

R(s) and *Y(s)* are two input signals in the above formula, where *R(s)* is a reference and *Y(s)* is the system's output. The weights for the proportional, integral, and derivative are K_P, K_i, and K_d respectively. The filter coefficient is *N*, and the controller output is. The set point weights on the proportional and derivative sections, respectively, are *PW* and *DW* in the equation.

4. The techniques projected for optimization

4.1. Sine-cosine optimization

The SCA algorithm was recently devised by Seyedali Mirjalili [27,28]. It is a stochastic population-based optimization approach that draws inspiration from the sine and cosine mathematical functions. This approach utilizes cyclic space create due to the mathematical model of sine and cosine for the search agent to amend their position while the equations for changing positions are given in Eqs. (2) and (3):

$$Y_j^{n+1} = Y_j^n + a_1 \sin\left(a_2\right) \times \left|a_3 P_j^n - Y_j^n\right|, \tag{2}$$

$$Y_j^{n+1} = Y_j^n + a_1 \cos\left(a_2\right) \times \left|a_3 P_j^n - Y_j^n\right|. \tag{3}$$

Y_j^n is current while Y_j^{n+1} are the next positions of the solution in the in the *j*th domain of the *n*th iteration. In the equation above a_1, a_2, and a_3 are the arbitrary numbers and represent the algorithm's major parameters. The endpoint point in the *j*th-dimension is P_j^n. Another parameter, a_4 is used to link the above equations. The algorithm will select one of the equations for updating the position of the investigating agent depending on the value of this parameter, which can be any number in the range [0, 1]. It is also provided in Eq. (4):

$$Y_j^{n+1} = \begin{cases} Y_j^n + a_1 sin\left(a_2\right) \times \left|a_3 P_j^n - Y_j^n\right| & \text{if } a_4 < 0.5 \\ Y_j^n + a_1 cos\left(a_2\right) \times \left|a_3 P_j^n - Y_j^n\right| & \text{if } a_4 < 0.5 \end{cases} \tag{4}$$

The subsequent position province that may be between the target and another will be determined by the parameter a_1. This parameter's goal is to balance this optimizer's exploitation and exploration, and its value may be calculated using the Eq. (5):

$$a_1 = b - n\frac{b}{N}, \tag{5}$$

N stands for the total iteration, *b* stands for the maximum number of iterations, and *n* represents the current iteration.

The parameter a_2 determines whether the search agent will travel in the direction of the global optima or moving elsewhere. The better outcome is attained by taking into account that the range of a_2 is between [-2 and 2], whereas [0, 2π] is the range of sine and cosine functions. The goal of parameter a_3 is to emphasise the target and will have any random value. It will stochastically emphasise the destination if it is more than 1 and vice-versa for less than 1.

4.2. Improved Sine-Cosine algorithm

Although in managing the real-time problems, SCA is quite competent of, there is still room for improvement in the algorithm, which would increase convergence rates, the capacity to not catch in neighboring optima, and the ability to strike a balance between exploration and exploitation. The updating strategy of its search agents is the cause of the aforementioned limitations of classical SCA. In the SCA, the majority of the search agents are directed toward the global optima and occasionally become stuck in the local optima, where they converge prematurely to the local optima. To address this, a novel strategy is shown here that primarily uses SCA/best-target (illustrated in Eqs. (6) and (7)) and SCA/rand-target to update the search agent's position (as shown is Eqs. (8) and (9)). The SCA's best-target search agent will help searchers go toward their current best position and conduct local searches close to the best search agent, which will intensify their quest for a solution. On the other hand, the SCA's random-target search agent will direct the search agents toward any point, leading to a greater exploration of the search space. The means from both schemes are merged in the following phase, as indicated in Eq. (10), and the resulting value is used to establish the new search agent. The suggested change to SCA will ensure that there is an implied balance between exploration and exploitation. Additionally, the algorithm's parameters will be lowered from its previous 4 to just 3. Eqs. (11), (12), and (13) demonstrate how these three parameters' values are determined, respectively.

$$Y_1 = Y_{best}^n + a_1 \sin\left(a_2\right)\times\left|a_3 Y_{rand}^n - Y_j^n\right|, \tag{6}$$

$$Y_2 = Y_{best}^n + a_1 \cos\left(a_2\right)\times\left|a_3 Y_{rand}^n - Y_j^n\right|, \tag{7}$$

$$Y_3 = Y_{rand}^n + a_1 \sin\left(a_2\right)\times\left|a_3 Y_{best}^n - Y_j^n\right|, \tag{8}$$

$$Y_4 = Y_{rand}^n + a_1 \cos\left(a_2\right)\times\left|a_3 Y_{best}^n - Y_j^n\right|, \tag{9}$$

$$Y_j^{n+1} = Mean\left(Y_1, Y_2, Y_3, Y_4\right), \tag{10}$$

$$a_1 = b\left(1-\frac{b}{N}\right), \tag{11}$$

$$a_2 = 2\times\pi\times rand\left(0,1\right), \tag{12}$$

$$a_3 = 2\times rand\left(0,1\right), \tag{13}$$

where n is the current iteration, b is a constant with a value of 2, the maximum iterations is N, and *rand (0,1)* stands for an arbitrary number generator which will be a number between 0 and 1.

Figure 3 displays the flow chart for the ISCA. The initialization, iteration, and termination phases make up the majority of the algorithm's steps. The algorithm will initialize the parameters like first set of search agents(solution), the number of search agents (c), the maximum number of iterations (N), number of variables to be tuned (d) with their lower (lb) bound and upper (ub). By averaging the four search agents produced by the suggested search strategies. The second phase will produce a single new search agent. The best agent thus far acquired will be chosen as the optimization problem's solution in the last phase.

4.3. Performance evaluation of the proposed approach

For the evaluation of the suggested techniques 13 standardized unimodal and multimodal benchmark functions is used; on the basis of which the supremacy of the suggested method is verified. For each benchmark function, each algorithm is independently executed 20 times. The aim of the optimization technique is to get the minimum value of the fitness value which will result into the most optimal solution of the problem. Table 1 displays the mean and standard deviations of fitness value for all the benchmark functions for the proposed and other algorithms. The technique which will attend the least average value of the fitness value will be considered better method compere to the other. The convergence curve comparison of PSO, SSA, SCA, ALO, and ISCA for various benchmark functions is shown in Figures 4 to 16. The convergence curve shows the value of the objective function(fitness value) versus the computation time during the minimization of the objective function. From the Figures 4 to 16 and Table 1 it can be observed that ISCA outperforms other approaches in seven functions $(F_1, F_2, F_3, F_4, F_7, F_{10}, F_{11},)$ whereas PSO outperforms other methods for (F_6, F_8, F_{12}) function, SCA outperforms other method for F_9 function, SSA outperform other method for F_5 and ALO outperforms other methods for F_{13} function, respectively.

Statistical analysis will be done for the further assessment of the superiority of the ISCA to other approaches. Wilcoxon Signed-Rank Test (WSRT) is the test which will be use for the statistical analysis. WSRT test is a nonparametric statistical test that compares two paired groups of data. The goal of the test is to determine if two or more sets of pairs are different from one another in a statistically significant manner. The Wilcoxon signed rank test assumes that there is information in the magnitudes and signs of the differences between paired observations. Depending upon the differences between data it assigns the sign +, -, ≈ which show the superior, inferior, and equal with to the compared one. In Table 2 ISCA has been compared statistically with ALO, SCA, SSA and PSO. As we can see from the Table 2 all the above mention techniques are inferior to the proposed ISCA for most of the cases.

As a result, when compared to the other approaches reviewed in this research, the suggested strategy performs better than others.

5. Objective function formulation

The main goal of LFC, if there is any interruption in the system is to (i) cancel out the frequency drift to zero (ii) The tie-line's exchange power is maintained at its scheduled value. The goal function for meeting the aforementioned objectives must be defined for each optimization issue in LFC. The goal function's frequency deviation and tie-line power deviation have been accumulated using a variety of criteria that have been presented in the literature. Among the objective function IAE, ISE, ITAE, and ISTE; ITAE (Integral of Time multiplied Absolute Error) is most utilized objective function as shown in the literature review [6,16]. As a result, the test system's objective function will be chosen to ITAE. The LFC's ITAE will be provided as given in Eq. (14).

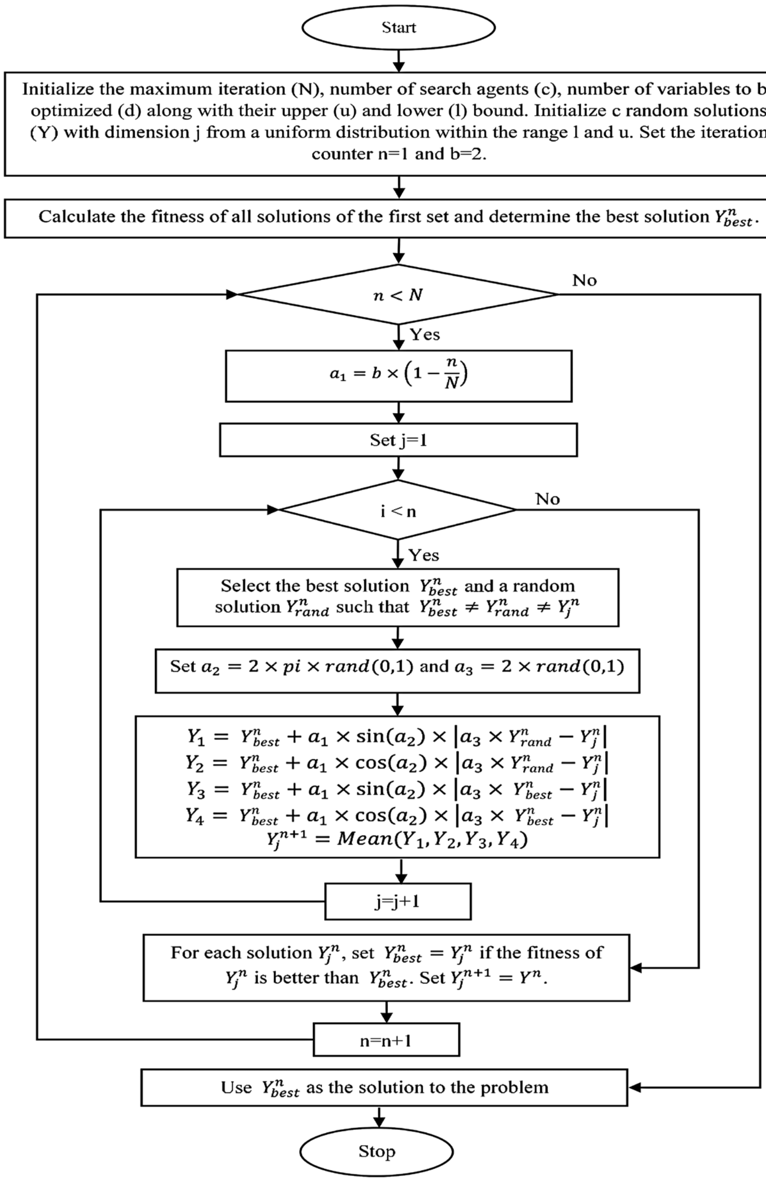

Figure 3. Flow chart of ISCA algorithm.

Table 1. Mean and standard deviation of fitness value for each benchmark function for algorithms.

	ISCA		SCA		ALO		SSA		PSO	
Function	**Mean**	**SD**	**Mean**	**SD**	**Mean**	**SD**	**Mean**	**SD**	**Mean**	**SD**
F_1	**8.752 E-22**	2.01E-21	6.02E-07	2.93E-06	3.89E-08	6.03E-08	7.84E-06	3.89E-05	5.81E-20	2.06E-18
F_2	**2.72E-13**	3.67E-13	6.83E-08	2.16E-07	9.63E-02	2.35E-01	2.78E-02	0.5617	2.53E-10	3.30E-10
F_3	**2.95E-12**	5.63E-11	1.2735	2.27168	4.42E-01	0.85962	5.92E-02	0.21321	0.003587	0.003801
F_4	**2.34E-08**	1.29E-06	0.7462	1.8481	6.22E-03	0.007331	6.23E-03	0.00361	0.00327	0.00434
F_5	**7.39926**	0.6528	8.9341	0.49967	8.7351	0.5886	8.945	0.6529	8.8256	0.7781
F_6	2.03E-02	0.2554	7.18E-02	0.3487	2.35E-08	7.78E-07	8.62E-06	3.87E-05	**8.73E-19**	3.36E-18
F_7	0.00575	0.005612	**0.00277**	0.00262	0.006421	0.0761	0.006342	0.02276	0.00468	0.00281
F_8	-2682.92	243.391	-2143.37	174.9436	-2438.56	493.0532	-2834.64	432.86	**-3678.06**	195.846
F_9	3.7614	4.3712	**1.6972**	3.1295	19.721	9.8786	25.298	7.4172	14.107	7.622
F_{10}	**3.00E-14**	6.42E-13	2.48E-07	5.47E-06	5.11E-05	9.16E-05	2.09E-02	2.09E-02	7.89E-09	4.28E-09
F_{11}	**0.05471**	0.063887	0.28418	0.29133	0.3314	0.3389	0.7381	0.6234	0.3437	0.3897
F_{12}	0.03619	0.02887	0.2487	0.06783	1.6931	2.2461	0.8167	1.7784	**2.22E-18**	3.39E-18
F_{13}	0.0997	0.0878	0.0422	0.08713	**3.16E-03**	0.00667	7.97E-03	0.00726	0.2237	0.2768

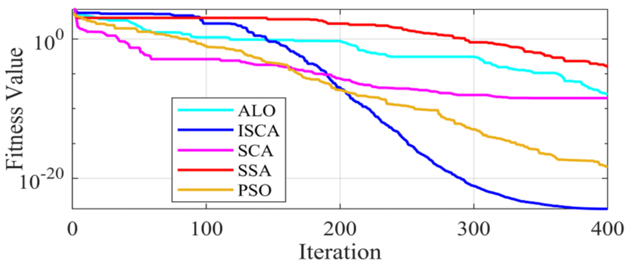

Figure 4. Convergence curve for F_1 function.

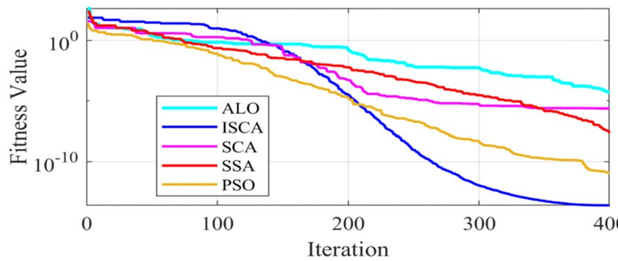

Figure 5. Convergence curve for F_2 function.

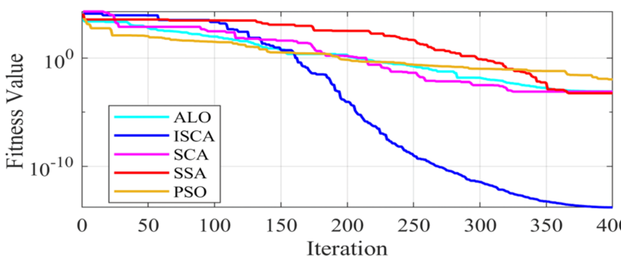

Figure 6. Convergence curve for F_3 function.

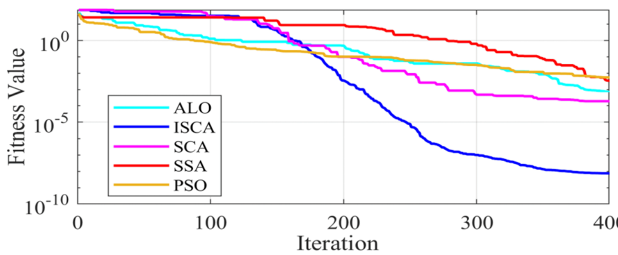

Figure 7. Convergence curve for F_4 function.

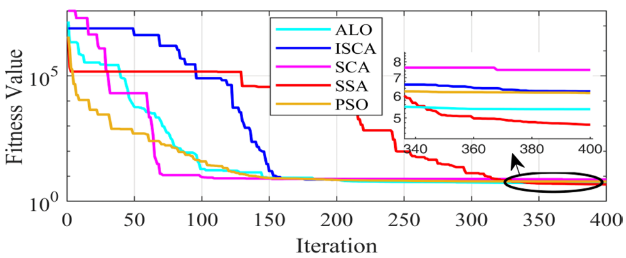

Figure 8. Convergence curve for F_5 function.

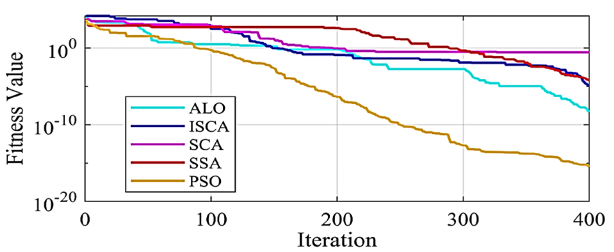

Figure 9. Convergence curve for F_6 function.

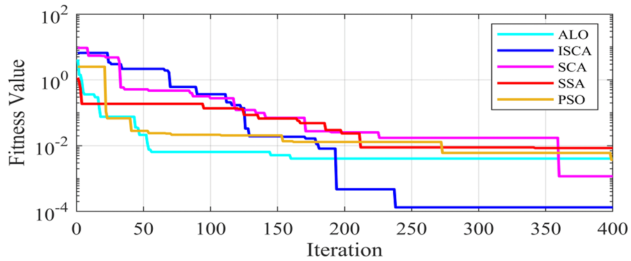

Figure 10. Convergence curve for F_7 function.

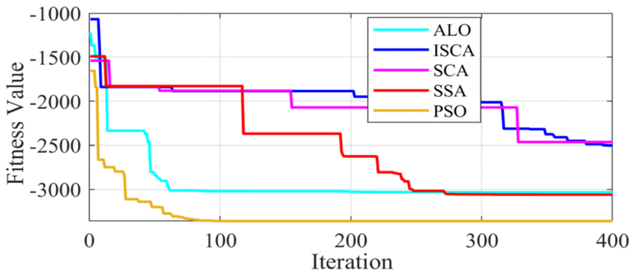

Figure 11. Convergence curve for F_8 function.

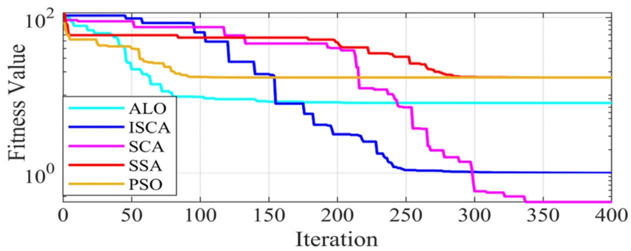

Figure 12. Convergence curve for F_9 function.

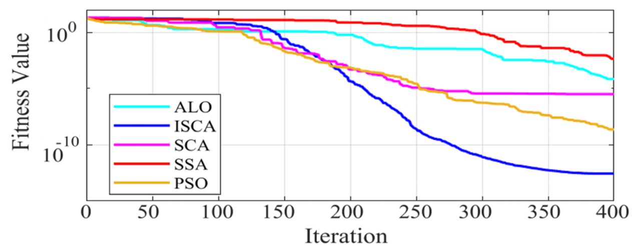

Figure 13. Convergence curve for F_{10} function.

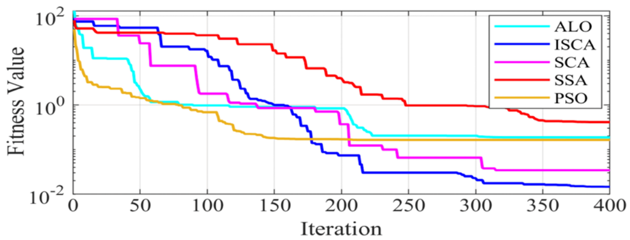

Figure 14. Convergence curve for F_{11} function.

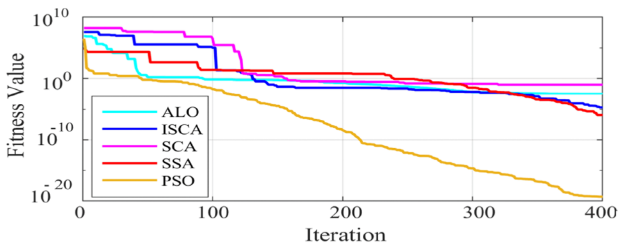

Figure 15. Convergence curve for F_{12} function.

Table 2. Wilcoxon signed rank test result on uni-model and multi-model function.

Algorithms	Functions												
	F_1	F_2	F_3	F_4	F_5	F_6	F_7	F_8	F_9	F_{10}	F_{11}	F_{12}	F_{13}
SCA	−	−	−	−	≈	−	−	≈	+	−	−	−	−
ALO	−	−	−	−	≈	+	−	+	−	−	−	−	+
SSA	−	−	−	−	≈	≈	−	+	−	−	−	≈	+
PSO	−	−	−	−	≈	+	−	+	−	−	−	+	−

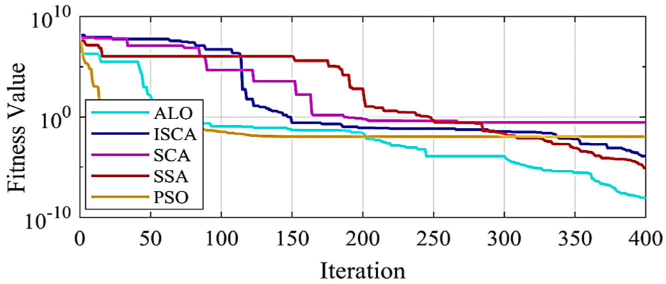

Figure 16. Convergence curve for F_{13} function.

$$J = ITAE = \sum_{i=1}^{NA} \int_0^{t_{sim}} \left(|\Delta f_i| + \sum_{\substack{j=1 \\ j \neq i}}^{NA} \left| \Delta P_{tie_{i-j}} \right| \right) .t.dt \,. \quad (14)$$

The accumulative fluctuation in tie-line power is shown by $\Delta P_{tie_{i-j}}$, Δf is drift in each region frequency, and t_{sim} is the simulation time period in Eq. (14). The constraint on the problem is the controller parameter boundary. By minimizing the objective function, the objective of the LFC can be achieved. So, the techniques which will get the least value of the objective function will give the best result.

Hence, the design problem may thus be described as an optimization problem:

Minimize J

For PID controller

$$K_{P_{\min}} \le K_P \le K_{P_{\max}} \,;\; K_{i_{\min}} \le K_i \le K_{i_{\max}} \,;$$
$$K_{d_{\min}} \le K_d \le K_{d_{\max}} \,;\; N_{\min} \le N \le N_{\max} \,.$$

For FOPID controller:

$$K_{P_{\min}} \le K_P \le K_{P_{\max}} \,; K_{i_{\min}} \le K_i \le K_{i_{\max}} \,;$$
$$K_{d_{\min}} \le K_d \le K_{d_{\max}} \,; \mu_{\min} \le \mu \le \mu_{\max} \,;$$
$$\lambda_{\min} \le \lambda \le \lambda_{\max} \,.$$

For 2-DOF-PID controller:

$$K_{P_{\min}} \le K_P \le K_{P_{\max}} \,; K_{i_{\min}} \le K_i \le K_{i_{\max}} \,;$$
$$K_{d_{\min}} \le K_d \le K_{d_{\max}} \,; N_{\min} \le N \le N_{\max} \,;$$
$$b_{\min} \le b \le b_{\max} \,; c_{\min} \le c \le c_{\max} \,.$$

6. Results and discussions

Numerous simulation studies have been conducted on the test system to identify the appropriate combination of the proposed algorithm and controller for a better result. Distinct kinds of research have been taken into consideration for this objective. Additionally, WSRT, the techniques for the statistical analysis have been used to indicate the approach that is inferior (-), superior (+), or equivalent (≈) to the suggested ISCA method for statistical evaluation of these techniques. Various controllers have been compared in Subsection 6.1 (Scenario 1) to determine which controller is best for the remaining research. Disturbances are provided in two areas in Subsection 6.2 (Scenario 2), and various algorithms have been evaluated as controller parameter optimizer and statistical analysis is performed for this section. Similar to Subsection 6.3, where disturbance is applied to all three areas (Scenario 3), several algorithms have again been compered as controller parameter optimizer, and statistical analysis has been utilized to determine which approach is best. The test system was regarded to include nonlinearities such GRC, GDB, and commutation delay in the final subsection (Scenario 4). Various algorithms were once again compered as controller parameter optimizer, and statistical analysis was conducted to determine the best algorithm.

6.1. Exhaustive inspection among controller

The literature review reveals that the PID controller variation are the preferred controller for implementation of proposed technique in LFC. 2-DOF-PID controller, fractional order PID controller (FOPID) and PID controller with filter (PIDF) are the three most popular controllers variation of PID controller. In order to discover the best controller for the current study, these controllers were first compared for the test system under consideration (an unequal three area system). In areas 1 and 2, a disturbance of 2% has been applied. The values of these controllers' parameters are listed in Table 3 after these parameters were optimized using the ISCA approach. Figure 17 depicts the tie-line power, frequency drift, and convergence curve of various controllers for this case. The LFC performance metric for these controllers is shown in Table 4. Therefore, it is evident from Table 4 and Figure 17 that the PIDF and FOPID are underperforming to 2-DOF -PID controller since it obtained least value of objective function and converges more quickly. Additionally, it has a minimum undershoot and lesser settling time for the frequency deviation and tie-line power. Hence the 2-DOF- PID controller has been adopted as the LFC controller for further research due of its benefits over other controllers.

Table 3. Parameter value of different controller tuned with ISCA.

Controller	Parameter value			ITAE
	Area-1	Area-2	Area-3	
2 DOF PID	$k_{p1} = 1.9868$ $k_{i1} = 1.9725$ $k_{d1} = 0.5204$ $n_1 = 121.23$ $b_1 = 0.2744$ $c_1 = 0.006479$	$k_{p2} = 0.20477$ $k_{i2} = 2$ $k_{d2} = 2.6058$ $n_2 = 9.4946$ $b_2 = 2.2531$ $c_2 = 0.00045$	$k_{p3} = 1.4549$ $k_{i3} = 0.72517$ $k_{d3} = 0.5801$ $n_3 = 23.4847$ $b_3 = 0.29992$ $c_3 = 0.1185$	ITAE=0.05626
FOPIDF	$k_{p1} = 1.613$ $k_{i1} = 1.859$ $l_1 = 1.001$ $k_{d1} = 0.62165$ $m_1 = 1.2036$	$k_{p2} = 0.04458$ $k_{i2} = 1.3358$ $l_2 = 1.0048$ $k_{d2} = 0.93426$ $m_2 = 0.06947$	$k_{p3} = 1.5125$ $k_{i3} = 0.16259$ $l_3 = 0$ $k_{d3} = 1.8401$ $m_3 = 1.6714$	ITAE=0.06903
PID	$k_{p1} = 0.6652$ $k_{i1} = 0$ $k_{d1} = 0.1763$ $n_1 = 199.8$	$k_{p2} = 1.999$ $k_{i2} = 1.999$ $k_{d2} = 1.142$ $n_2 = 199.78$	$k_{p3} = 2$ $k_{i3} = 1.6447$ $k_{d3} = 0.9859$ $n_3 = 63.1186$	ITAE=0.1034

Table 4. Transient parameter of LFC for controllers for Scenario 1.

		Controller		
		2-DOF-PID	FOPID	PID
$\boldsymbol{\Delta F_1}$	Maximum deviation	-0.008648	-0.0135	-0.01753
	Settling time	6.295	7.765	8.619
$\boldsymbol{\Delta F_2}$	Maximum deviation	-0.006594	-0.01228	-0.0142
	Settling time	4.739	6.445	6.63
$\boldsymbol{\Delta F_3}$	Maximum deviation	-0.007859	-0.00173	-0.00245
	Settling time	4.447	6.655	6.972
$\boldsymbol{\Delta P_{1-2}}$	Maximum deviation	-16.53×10^{-5}	-45.92×10^{-5}	-53.77×10^{-5}
	Settling time	8.265	9.133	9.993
$\boldsymbol{\Delta P_{2-3}}$	Maximum deviation	-7.311×10^{-5}	-27.87×10^{-5}	-41.47×10^{-5}
	Settling time	7.993	8.997	9.898
$\boldsymbol{\Delta P_{3-1}}$	Maximum deviation	20.15×10^{-5}	64.67×10^{-5}	85.72×10^{-5}
	Settling time	4.997	6.652	7.991

6.2. Exhaustive inspection among optimization techniques when disturbances are in two area

In this phase, ISCA is used to fine-tune the controller parameters in order to verify the applicability of the suggested method. When a 2% disturbance has been delivered to both area-1 and area-2, the test system is simulated with 2-DOF-PID controller. The outcomes are contrasted with a few recently popular algorithms, including PSO, SSA, SCA, and ALO. In Table 5, the controller parameter's value is listed with all the above mention algorithm. Transient reactions of the test system and the convergence curve are shown in Figure 18. Plotting the ISCA convergence curve against the SCA, ALO, SSA, and PSO reveals that ISCA converges more quickly and achieves the lowest objective function (ITAE value). The transient metrics of the LFC for various algorithms in this situation are shown in Table 6. As it can been seen that ISCA have least value of settling time, minimum peak undershoot compare to other. As a result, it is clear from Figure 18 and Table 6 that ISCA outperforms all other optimization methods.

For the statistical analysis SCA, SSA, ALO PSO, and ISCA simulate the LFC controller parameters 20 times in total to more evaluate the effectiveness of ISCA in optimising the controller parameters. The mean and standard deviation of the ITAE for each approach are shown in Table 7. The ISCA achieves the lowest mean value of the ITAE when compared to other approaches. Additionally, WSRT has been used to evaluate these strategies statistically. Results of the Wilcoxon signed-rank test is shown in Table 8 for this case. It can see that all the technique are inferior to the ISCA. Hence it can be said that ISCA is better techniques to other for this test system in this scenario.

Table 5. Controller parameter with each algorithm for Scenario 2.

Algorithm	PID controller parameter value			ITAE
	Area-1	Area-2	Area-3	
ISCA	$k_{p1}=2$ $k_{i1}=2$ $k_{d1}=2$ $n_1=200$ $b_1=4.5961$ $c_1=0.5$	$k_{p2}=2$ $k_{i2}=2$ $k_{d2}=2$ $n_2=200$ $b_2=5$ $c_2=0$	$k_{p3}=1.2038$ $k_{i3}=0$ $k_{d3}=1.9987$ $n_3=181.43$ $b_3=4.9979$ $c_3=0.005652$	ITAE=0.018985
SCA	$k_{p1}=1.9381$ $k_{i1}=2$ $k_{d1}=1.9287$ $n_1=111.97$ $b_1=2.1224$ $c_1=0.38428$	$k_{p2}=0.35707$ $k_{i2}=2$ $k_{d2}=0.8104$ $n_2=111.84$ $b_2=2.0047$ $c_2=0.32901$	$k_{p3}=0.91383$ $k_{i3}=1.4298$ $k_{d3}=0.80135$ $n_3=93.548$ $b_3=1.0214$ $c_3=0.288$	ITAE=0.02647
ALO	$k_{p1}=1.2112$ $k_{i1}=1.3913$ $k_{d1}=0.61201$ $n_1=80.69$ $b_1=1.1812$ $c_1=0.39736$	$k_{p2}=0.41567$ $k_{i2}=2$ $k_{d2}=0.72902$ $n_2=200$ $b_2=0.4079$ $c_2=0.40261$	$k_{p3}=0.58772$ $k_{i3}=0$ $k_{d3}=0.54525$ $n_3=171.59$ $b_3=0$ $c_3=0.09515$	ITAE=0.034557
SSA	$k_{p1}=1.2208$ $k_{i1}=2$ $k_{d1}=1.642$ $n_1=54.433$ $b_1=4.5339$ $c_1=0.46087$	$k_{p2}=0.34802$ $k_{i2}=2$ $k_{d2}=0.49874$ $n_2=186.45$ $b_2=1.378$ $c_2=0.2794$	$k_{p3}=1.1609$ $k_{i3}=1.8442$ $k_{d3}=1.4132$ $n_3=72.93$ $b_3=0.25395$ $c_3=0.25372$	ITAE=0.044409
PSO	$k_{p1}=1.8655$ $k_{i1}=1.4277$ $k_{d1}=0.23492$ $n_1=182.09$ $b_1=0.1840$ $c_1=0.12477$	$k_{p2}=0.3438$ $k_{i2}=1.8581$ $k_{d2}=0.56365$ $n_2=148.67$ $b_2=3.506$ $c_2=0.08033$	$k_{p3}=0.97596$ $k_{i3}=1.2288$ $k_{d3}=0.3863$ $n_3=130.09$ $b_3=0.11731$ $c_3=0.26697$	ITAE=0.088735

Table 6. Transient metrics of the LFC for various algorithms for Scenario 2.

		Algorithm				
		ISCA	SCA	SSA	ALO	PSO
$\Delta \boldsymbol{F_1}$	Maximum deviation	-0.00597	-0.00623	-0.0132	-0.00902	-0.01771
	Settling time	5.617	8.723	8.931	8.923	9.173
$\Delta \boldsymbol{F_2}$	Maximum deviation	-0.00521	-0.00863	-0.0011	-0.0132	-0.0139
	Settling time	9.315	12.72	14.82	13.91	15.13
$\Delta \boldsymbol{F_3}$	Maximum deviation	-0.01339	-0.01349	-0.0221	-0.0164	-0.0231
	Settling time	10.73	11.31	14.92	13.42	15.01
$\Delta \boldsymbol{P_{1-2}}$	Maximum deviation	-5.01×10^{-4}	-10.23×10^{-4}	-13.94×10^{-4}	-13.23×10^{-4}	-15.02×10^{-4}
	Settling time	9.135	13.65	14.61	13.91	15.02
$\Delta \boldsymbol{P_{2-3}}$	Maximum deviation	-0.00031	-0.00131	-0.00197	-0.0017	-0.00221
	Settling time	7.79	14.12	15.21	16.23	17.19
$\Delta \boldsymbol{P_{3-1}}$	Maximum deviation	0.00791	0.00163	0.00239	0.00231	0.00249
	Settling time	11.73	12.11	15.11	13.91	15.23

Table 7. Fitness values comparison of different optimization techniques in Scenario 2 (values in bold shows best value).

	ISCA Mean$\pm$ Std. Dev	**SCA** Mean$\pm$ Std Dev	**ALO** Mean$\pm$ Std.Dev	**SSA** Mean$\pm$ Std. Dev	**PSO** Mean$\pm$ Std. Dev
Fitness value	**0.0231175** $\pm$ **0.008800165**	0.031108 $\pm$ 0.012946	0.041118 $\pm$ 0.016742	0.068661 $\pm$ 0.018436	0.116889 $\pm$ 0.017588

Table 8. WSRT results of different optimization techniques in Scenario 2.

	SCA	ALO	SSA	PSO
Fitness value	–	–	–	–

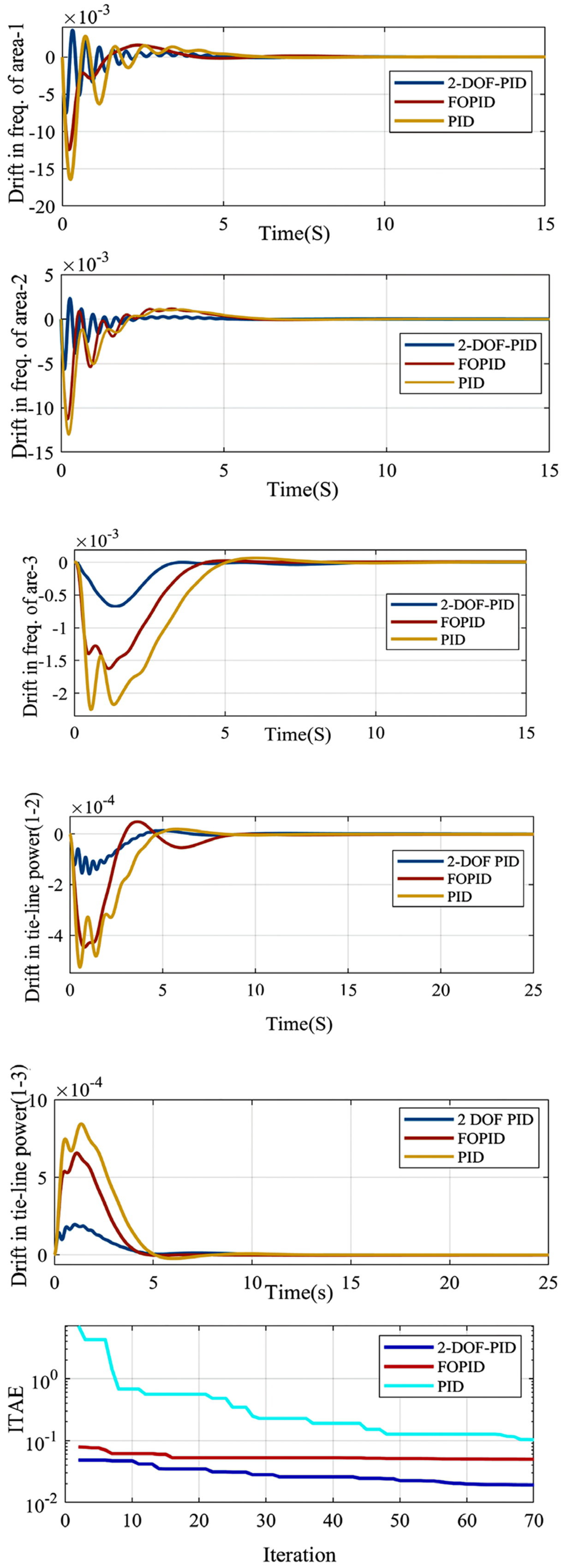

Figure 17. Drift responses of all area frequency and tie-line and convergence curve of controllers for Scenario 1.

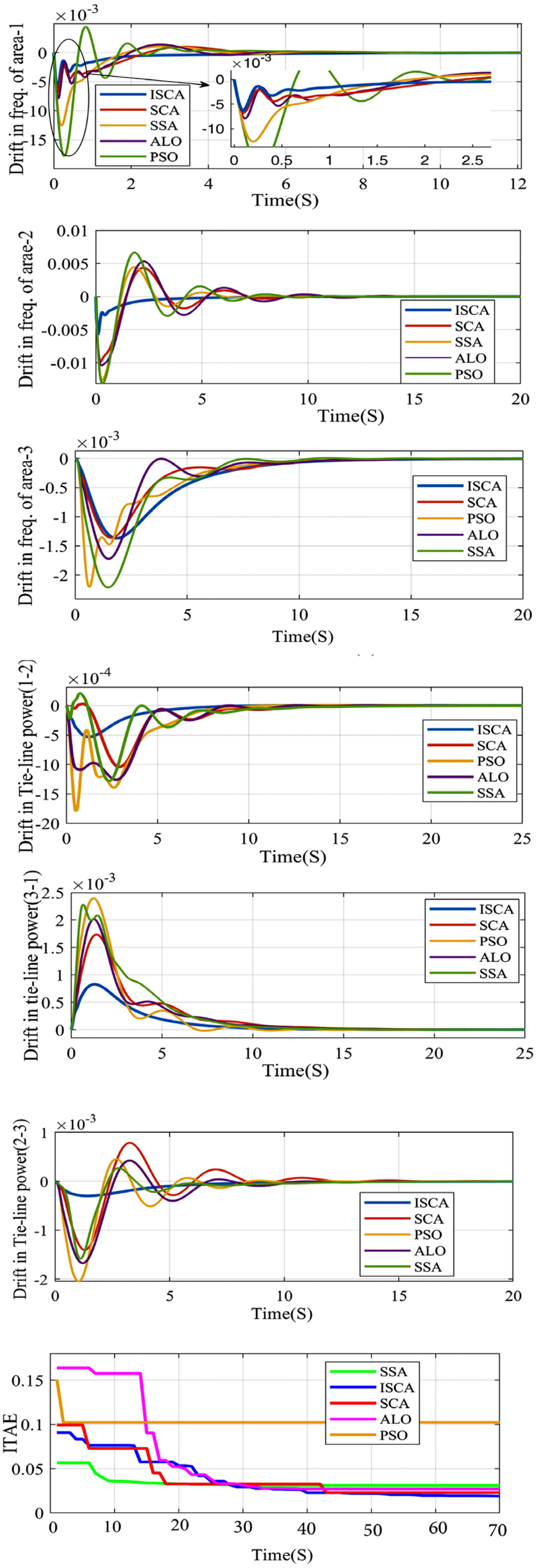

Figure 18. Drift responses of all area frequency and tie-line and convergence curve of algorithms for Scenario 2.

6.3. Exhaustive inspection among optimization techniques when interruption is in each area

In this segment, the improved sin-cosine algorithm has been used to optimize the controller parameter in order to verify its suitability. A 2% disturbance given to each section of the test system simulates the 2-DOF-PID controlled test system. Here, the results are contrasted with a few recently popular algorithms, including PSO, SSA, SCA, and ALO. Table 9 lists the controller parameter values for various methodologies, and Figure 19 shows the test system's convergence curve and transient reactions. Plotting the ISCA convergence curve against the SCA, ALO, SSA, and PSO reveals that ISCA converges more quickly and achieves the lowest objective function (ITAE value). Table 10 lists the transient metrics for various methods in this situation. As it can been seen that ISCA have least value of settling time, minimum peak undershoot compare to other for the frequency and tie-line of each area. As a result, it is clear from Figure 19 and Table 10 that ISCA outperforms all other optimization methods.

For the statistical analysis ISCA, PSO, SSA, ALO, and SCA simulate the LFC controller parameters 20 times in total to further evaluate the effectiveness of ISCA in optimising the controller parameters. The mean and standard deviation of the ITAE for each approach are shown in Table 11. The ISCA achieves the lowest mean value of the ITAE when compared to other approaches. Additionally, WSRT has been used to evaluate these strategies statistically. Table 12 presents the WSRT findings. It can see that all the technique are inferior to the ISCA. Hence it can be said that ISCA is better techniques to other for this test system in this scenario.

6.4. Exhaustive inspection among optimization techniques with including physical restrain

Test system has been modifies in this segment and several physical restrictions such as reheated turbine, GRC, communication delay and GDB takes into account. Since the practical power system exhibits this kind of nonlinearity, the modified system is very similar to the practical system after taking these constraints into account. As the complexity of power system in increasing with time in the deregulated environment communication time delay became a major challenge in LFC analysis. This time delay degrades the performance of power system and potentially causing the system to become unstable. Generation Rate Constant (GRC) imposes a realistic restriction on the generation of power systems due to the existence of thermal and mechanical limitations. Only if a power system includes a steam plant may power generation alter at a defined maximum pace. The Governor Dead Band (GDB) is the entire amount of continuous speed fluctuation under which the valve position stays optimum. GDB is typically represent by backlash type of non-linearity. To study the significance effect of aforesaid nonlinearity and to identify the stability of the system 1% of step load disturbance enforced in area-1.

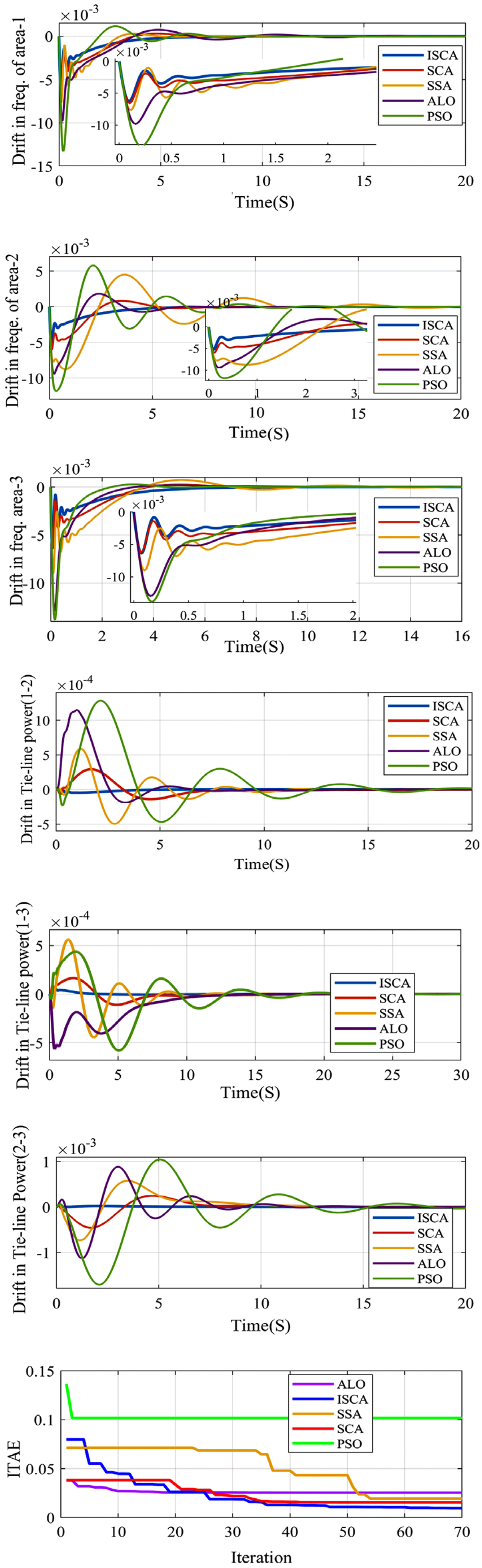

Figure. 19. Drift responses of all area frequency and tie-line and convergence curve of algorithms for Scenario 3.

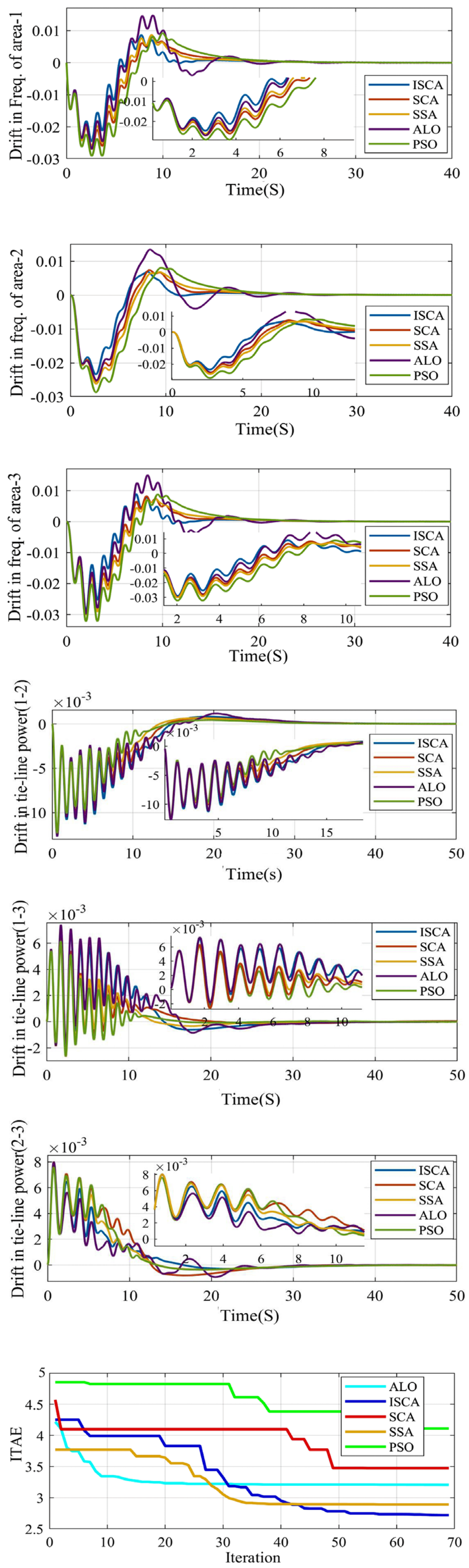

Figure. 20. Drift responses of all area frequency and tie-line and convergence curve of algorithms for Scenario 4.

Each area of the system has taken into account the 40 ms communication time, GRC of 3% pu, and GDB of 0.036 pu. For this 2-DOF-PID controlled system, the suggested algorithm and other algorithms have been examined, and the controller parameters using these methods are shown in Table 13. Figure 20 shows the dynamic responses and convergence curve for this situation. The transient parameter is displayed in Table 14. The transient parameter, drift response and convergence curve all support the conclusion that the suggested ISCA technique has significantly higher tuning efficacy than existing techniques.

For the statistical analysis SCA, ALO, PSO, SSA, and ISCA simulate the LFC controller parameters 20 times in total to more evaluate the effectiveness of ISCA in optimising the controller parameters. The mean and standard deviation of the ITAE for each approach are shown in Table 15. The ISCA achieves the lowest mean value of the ITAE when compared to other approaches. Additionally, WSRT has been used to evaluate these strategies statistically. Results of the Wilcoxon signed-rank test for this scenario is shown in Table 16. It can see that all the technique are inferior to the ISCA. Hence it can be said that ISCA is better techniques to other for this test system in this scenario.

7. Conclusion

In this study an Improved SCA (ISCA) has been proposed as the tuning tool for the Load Frequency Control (LFC) controller of three area unequal power system. The projected scheme benefits from the exploration expertise of SCA/rand-target search agent and the exploitation expertise of SCA/best-target search agent, with maintaining a balance between exploitation and exploration. The 2-DOF-PID controller emerged as the superior one when certain controllers were first compared to one another for the test system under consideration. Additionally, this controller is employed as a load frequency controller for various analyses. For this test system, the tuning capability of ISCA is evaluated under some scheme like as disturbance in each areas, disturbance in two areas and the test system with various non-linearity. Additionally, the ISCA's performance is contrasted with that of a few other promising algorithms. Additionally, statistical analysis has been used to test the usefulness of the suggested strategy in various settings. After assessment of the above result, it is concluded that the suggested method outperforms other approaches such as SCA, SSA, PSO and ALO in terms of superior rate of convergence, obtain the smallest value objective function, minimal undershoot and smallest settling time. Therefore, it can be inferred that the recommended strategy might be used to address LFC issues that arise in the actual world.

Funding

This research did not receive any specific grant from funding agencies in the public, commercial, or not-for-profit sectors.

Conflicts of interest

The authors declare that they have no known competing financial interests or personal relationships that could have appeared to influence the work reported in this paper.

Authors contribution statement

Neelesh Kumar Gupta: Conceptualization; Investigation; Methodology; Roles/writing-original draft. Manoj Kumar Kar: Methodology; Validation. Arun Kumar Singh: Supervision, writing-review and editing.

Table 9. Controller parameter with each algorithm for Scenario 3.

Algorithm	PID controller parameters value			ITAE
	Area-1	Area-2	Area-3	
ISCA	$k_{p1} = 2$ $k_{i1} = 2$ $k_{d1} = 2$ $n_1 = 200$ $b_1 = 5$ $c_1 = 0.5$	$k_{p2} = 2$ $k_{i2} = 2$ $k_{d2} = 2$ $n_2 = 200$ $b_2 = 5$ $c_2 = 0.5$	$k_{p3} = 2$ $k_{i3} = 2$ $k_{d3} = 1.9936$ $n_3 = 181.43$ $b_3 = 4.9979$ $c_3 = 0$	ITAE=0.03691
SCA	$k_{p1} = 1.5531$ $k_{i1} = 2$ $k_{d1} = 1.9374$ $n_1 = 138.24$ $b_1 = 4.6787$ $c_1 = 0.47987$	$k_{p2} = 0.75224$ $k_{i2} = 1.9408$ $k_{d2} = 1.8258$ $n_2 = 87.025$ $b_2 = 3.5846$ $c_2 = 0.49496$	$k_{p3} = 1.2895$ $k_{i3} = 1.952$ $k_{d3} = 1.8525$ $n_3 = 187.43$ $b_3 = 4.9864$ $c_3 = 0.37147$	ITAE=0.05882
ALO	$k_{p1} = 2$ $k_{i1} = 2$ $k_{d1} = 1.7106$ $n_1 = 54.208$ $b_1 = 4.0216$ $c_1 = 0.5$	$k_{p2} = 1.0883$ $k_{i2} = 1.8389$ $k_{d2} = 0.92595$ $n_2 = 200$ $b_2 = 0.2336$ $c_2 = 0.0012$	$k_{p3} = 2$ $k_{i3} = 1.398$ $k_{d3} = 0.52057$ $n_3 = 200$ $b_3 = 0$ $c_3 = 0$	ITAE=0.1025
SSA	$k_{p1} = 0.75943$ $k_{i1} = 1.9979$ $k_{d1} = 0.57757$ $n_1 = 116.87$ $b_1 = 4.99$ $c_1 = 0.11099$	$k_{p2} = 0.45169$ $k_{i2} = 1.9994$ $k_{d2} = 0.63028$ $n_2 = 171.81$ $b_2 = 0.10286$ $c_2 = 0.35034$	$k_{p3} = 1.7224$ $k_{i3} = 1.9899$ $k_{d3} = 0.42088$ $n_3 = 156.79$ $b_3 = 0.21609$ $c_3 = 0.27511$	ITAE=0.08561
PSO	$k_{p1} = 1.6624$ $k_{i1} = 1.7113$ $k_{d1} = 0.91464$ $n_1 = 199.9$ $b_1 = 1.4663$ $c_1 = 0.41186$	$k_{p2} = 0.24332$ $k_{i2} = 1.2201$ $k_{d2} = 1.2259$ $n_2 = 141.16$ $b_2 = 1.0349$ $c_2 = 0.29421$	$k_{p3} = 0.1.5073$ $k_{i3} = 1.3607$ $k_{d3} = 1.2048$ $n_3 = 62.15$ $b_3 = 1.2758$ $c_3 = 0.24801$	ITAE=0.2753

Table 10. Transient metrics of the LFC for various algorithms for Scenario 3.

		Algorithm				
		ISCA	SCA	SSA	ALO	PSO
ΔF_1	Maximum deviation	-0.00593	-0.00612	-0.0073	-0.00913	-0.00153
	Settling time	7.42	8.32	7.83	14.42	14.92
ΔF_2	Maximum deviation	-0.00523	-0.00542	-0.00917	-0.00853	-0.0136
	Settling time	7.31	12.36	13.91	20	17.71
ΔF_3	Maximum deviation	-0.00611	-0.00613	-0.0083	-0.0125	-0.014
	Settling time	8.13	9.34	14.11	10.32	14.92
ΔP_{1-2}	Maximum deviation	-0.62×10^{-4}	-2.12×10^{-4}	-5.21×10^{-4}	-2.32×10^{-4}	-4.97×10^{-4}
	Settling time	10.31	13.52	13.72	14.11	19.74
ΔP_{2-3}	Maximum deviation	-0.000012	-0.000045	-0.000067	-0.00012	-0.00017
	Settling time	4.22	9.321	11.91	12.91	19.63
ΔP_{3-1}	Maximum deviation	-0.9×10^{-4}	-1.12×10^{-4}	-5.89×10^{-4}	-4.23×10^{-4}	-5.92×10^{-4}
	Settling time	8.23	10.32	14.12	14.43	19.52

Table 11. Fitness values comparison of different optimization techniques in Scenario-3 (Values in bold shows best value).

	ISCA Mean± Std. Dev	SCA Mean± Std.Dev	ALO Mean± Std.Dev	SSA Mean± Std. Dev	PSO Mean± Std. Dev
Fitness value	**0.01433026 ± 0.002703**	0.016443 ± 0.003433374	0.027976 ± 0.006409	0.021504 ± 0.00409	0.066433 ± 0.011953

Table 12. WSRT results of different optimization techniques in Scenario 3.

	SCA	ALO	SSA	PSO
Fitness value	–	–	–	–

Table 13. Controller parameter with each algorithm for Scenario 4.

Algorithm	PID controller parameters value			ITAE
	Area-1	Area-2	Area-3	
ISCA	$k_{p1} = 5.8949$ $k_{i1} = 9.46219$ $k_{d1} = 9.526902$ $n_1 = 53.7972$ $b_1 = 6.075843$ $c_1 = 0.16406$	$k_{p2} = 1.87254$ $k_{i2} = 5.9328$ $k_{d2} = 7.70743$ $n_2 = 50.47483$ $b_2 = 8.70567$ $c_2 = 0.06931$	$k_{p3} = 7.6226$ $k_{i3} = 9.7457$ $k_{d3} = 3.1165$ $n_3 = 129.8511$ $b_3 = 1.3083$ $c_3 = 0.18791$	ITAE=2.729
SCA	$k_{p1} = 5.09944$ $k_{i1} = 4.79296$ $k_{d1} = 3.993$ $n_1 = 86.3914$ $b_1 = 3.62701$ $c_1 = 0$	$k_{p2} = 4.56491$ $k_{i2} = 8.3516$ $k_{d2} = 7.7609$ $n_2 = 57.8992$ $b_2 = 2.8328$ $c_2 = 0.2083$	$k_{p3} = 6.90364$ $k_{i3} = 8.17205$ $k_{d3} = 8.7362$ $n_3 = 175.0415$ $b_3 = 6.52147$ $c_3 = 0.22287$	ITAE=3.4481
ALO	$k_{p1} = 2.6619$ $k_{i1} = 6.94081$ $k_{d1} = 4.9067$ $n_1 = 45.222$ $b_1 = 6.3337$ $c_1 = 0$	$k_{p2} = 0.68168$ $k_{i2} = 1.76264$ $k_{d2} = 2.84776$ $n_2 = 50.9051$ $b_2 = 0.00012$ $c_2 = 0.0613$	$k_{p3} = 3.22689$ $k_{i3} = 8.7165$ $k_{d3} = 4.24915$ $n_3 = 85.599$ $b_3 = 6.07698$ $c_3 = 0.00179$	ITAE=3.2122
SSA	$k_{p1} = 5.81720$ $k_{i1} = 7.810915$ $k_{d1} = 6.0790$ $n_1 = 55.92486$ $b_1 = 4.4488$ $c_1 = 0.19217$	$k_{p2} = 2.13477$ $k_{i2} = 4.10888$ $k_{d2} = 7.4918$ $n_2 = 79.5802$ $b_2 = 8.21545$ $c_2 = 0.12585$	$k_{p3} = 4.291598$ $k_{i3} = 6.57509$ $k_{d3} = 6.49455$ $n_3 = 119.1325$ $b_3 = 4.9131$ $c_3 = 0.28038$	ITAE=2.8918
PSO	$k_{p1} = 3.1957$ $k_{i1} = 9.3822$ $k_{d1} = 4.3081$ $n_1 = 35.8053$ $b_1 = 5.3555$ $c_1 = 0.3906$	$k_{p2} = 4.5849$ $k_{i2} = 6.2750$ $k_{d2} = 4.7443$ $n_2 = 108.6032$ $b_2 = 8.9004$ $c_2 = 0.4003$	$k_{p3} = 7.9975$ $k_{i3} = 4.7693$ $k_{d3} = 8.8635$ $n_3 = 137.9072$ $b_3 = 5.2329$ $c_3 = 0.4884$	ITAE=4.0550

Table 14. Transient metrics of the LFC for various algorithms for Scenario 4.

		Algorithm				
		ISCA	SCA	SSA	ALO	PSO
ΔF_1	Maximum deviation	-0.0217	-0.0262	-0.0261	-0.0261	-0.0291
	Settling time	23.42	26.15	25.19	27.56	27.12
ΔF_2	Maximum deviation	-0.0228	-0.0263	-0.0269	-0.0258	-0.0292
	Settling time	16.24	20.64	23.91	29.17	25.12
ΔF_3	Maximum deviation	-0.0278	-0.0296	-0.0308	-0.0302	-0.0328
	Settling time	16.61	18.48	20.53	28.47	26.89
ΔP_{1-2}	Maximum deviation	-0.01221	-0.01379	-0.01380	-0.01479	-0.01481
	Settling time	31.15	34.31	38.45	35.61	38.45
ΔP_{2-3}	Maximum deviation	0.00688	0.00731	0.00736	0.0780	0.00755
	Settling time	32.87	35.15	37.83	36.43	39.15
ΔP_{3-1}	Maximum deviation	0.00618	0.00643	0.00642	0.0078	0.00628
	Settling time	32.64	37.49	36.19	38.34	39.89

Table 15. Fitness values comparison of different optimization techniques in Scenario 4 (Values in bold shows best value).

	ISCA Mean± Std. Dev	SCA Mean± Std. Dev	ALO Mean± Std. Dev	SSA Mean± Std. Dev	PSO Mean± Std. Dev
Fitness value	**2.76455 ± 0.030228369**	3.303025 ± 0.175311	3.043113 ± 0.226013	2.9268 ± 0.339249	4.0440 ± 0.639504

Table 16. WSRT results of different optimization techniques in Scenario 4.

	SCA	ALO	SSA	PSO
Fitness value	–	–	–	–

References

1. Kundur, P., *Power System Stability and Control*. 8th Ed., New Delhi: Tata McGraw-Hill; 2009. [2]" (n.d.).

2. Pandey, S.K., Mohanty, S.R., and Kishor, N. "A literature survey on load-frequency control for conventional and distribution generation power systems", *Renew. Sustain. Energy Rev.*, **25**, pp. 318–334 (2013). https://doi.org/10.1016/j.rser.2013.04.029

3. Shayeghi, H., Jalili, A., and Shayanfar, H.A. "Multi-stage fuzzy load frequency control using PSO", *Energy Convers. Manag.*, **49**(10), pp. 2570–2580 (2008). https://doi.org/10.1016/j.enconman.2008.05.015

4. Hote, Y.V. and Jain, S. "PID controller design for load frequency control: Past, Present and future challenges", *IFAC-PapersOnLine*, **51**(4), pp. 604–609 (2018). https://doi.org/10.1016/j.ifacol.2018.06.162

5. Pain, S. and Acharjee, P. "Multiobjective optimization of load frequency control using PSO", *International Journal of Emerging Technology and Advanced Engineering*, **4**(7), pp. 16–22 (2014).

6. Sahu, R.K., Panda, S., and Padhan, S. "Optimal gravitational search algorithm for automatic generation control of interconnected power systems", *Ain Shams Eng. J.*, **5**(3), pp. 721–733 (2014). https://doi.org/10.1016/j.asej.2014.02.004

7. Satheeshkumar, R. and Shivakumar, R. "Ant lionoptimization approach for load frequency control of multi-area interconnected power systems", *Circuits Syst.*, **07**(09), pp. 2357–2383 (2016). DOI: 10.4236/cs.2016.79206

8. Arya, Y. "Automatic generation control of two-area electrical power systems via optimal fuzzy classical controller", *J. Franklin Inst.*, **355**(5), pp. 2662–2688 (2018). https://doi.org/10.1016/j.jfranklin.2018.02.004

9. Sahu, R.K., Panda, S., and Rout, U.K. "DE optimized parallel 2-DOF PID controller for load frequency control of power system with governor dead-band nonlinearity", *Int. J. Electr. Power Energy Syst.*, **49**(1), pp. 19–33 (2013). https://doi.org/10.1016/j.ijepes.2012.12.009

10. Latif, A., Hussain, S.M.S., Das, D.C., et al. "A review on fractional order (FO) controllers' optimization for load frequency stabilization in power networks", *Energy Reports*, **7**, pp. 4009–4021 (2021). https://doi.org/10.1016/j.egyr.2021.06.088

11. Taher, S.A., Hajiakbari Fini, M., and Falahati Aliabadi, S. "Fractional order PID controller design for LFC in electric power systems using imperialist competitive algorithm", *Ain Shams Eng. J.*, **5**(1), pp. 121–135 (2014). https://doi.org/10.1016/j.asej.2013.07.006

12. Delassi, A., Arif, S., and Mokrani, L. "Load frequency control problem in interconnected power systems using robust fractional PIλD controller", *Ain Shams Eng. J.*, **9**(1), pp. 77–88 (2018). https://doi.org/10.1016/j.asej.2015.10.004

13. Zamani, A., Barakati, S.M., and Yousofi-Darmian, S. "Design of a fractional order PID controller using GBMO algorithm for load–frequency control with governor saturation consideration", *ISA Trans.*, **64**, pp. 56–66 (2016). https://doi.org/10.1016/j.isatra.2016.04.021

14. Saurabh, K., Gupta, N.K., and Singh, A.K. "Fractional order controller design for load frequency control of single area and two area system", *2020 7th Int. Conf. Signal Process. Integr. Networks, SPIN 2020*, pp. 531–536 (2020). DOI: 10.1109/SPIN48934.2020.9070993

15. Jagatheesan, K., Anand, B., Dey, K.N., et al. "Performance evaluation of objective functions in automatic generation control of thermal power system using ant colony optimization technique-designed proportional-integral-derivative controller", *Electr. Eng.*, **100**(2), pp. 895–911 (2018). https://doi.org/10.1007/s00202-017-0555-x

16. Hasanien, H.M. and El-Fergany, A.A. "Salp swarm algorithm-based optimal load frequency control of hybrid renewable power systems with communication delay and excitation cross-coupling effect", *Electr. Power Syst. Res.*, **176**, 105938 (2019). https://doi.org/10.1016/j.epsr.2019.105938

17. Kumari, S. and Shankar, G. "A novel application of salp swarm algorithm in load frequency control of multi-area power system", *Proc. 2018 IEEE Int. Conf. Power Electron. Drives Energy Syst. PEDES 2018*, **3**, pp. 1–5 (2018). DOI: 10.1109/PEDES.2018.8707635

18. Sharma, M., Prakash, S., Saxena, S., et al. "Optimal fractional-order tilted-integral-derivative controller for frequency stabilization in hybrid power system using salp swarm algorithm", *Electr. Power Components Syst.*, **48**(18), pp. 1912–1931 (2021). https://doi.org/10.1080/15325008.2021.1906792

19. Mohapatra, T.K., Dey, A.K., and Sahu, B.K. "Employment of quasi oppositional SSA-based two-degree-of-freedom fractional order PID controller for AGC of assorted source of generations", *IET Gener. Transm. Distrib.*, **14**(17), pp. 3365–3376 (2020). https://doi.org/10.1049/iet-gtd.2019.0284

20. AH, G.H. and Li, Y.Y. "Ant lion optimized hybrid intelligent PID-based sliding mode controller for frequency regulation of interconnected multi-area power systems", *Trans. Inst. Meas. Control*, **42**(9), pp. 1594–1617 (2020). https://doi.org/10.1177/0142331219892728

21. Fathy, A. and Kassem, A.M. "Antlion optimizer-ANFIS load frequency control for multi-interconnected plants comprising photovoltaic and wind turbine", *ISA Trans.*, **87**, pp. 282–296 (2019). https://doi.org/10.1016/j.isatra.2018.11.035

22. Sahu, P.C., Prusty, R.C., and Sahoo, B.K., "Modified sine cosine algorithm-based fuzzy-aided PID controller for automatic generation control of multiarea power systems", *Soft Comput.*, **24**(17), pp. 12919–12936 (2020). https://doi.org/10.1007/s00500-020-04716-y

23. Khokhar, B., Dahiya, S., and Parmar, K.P.S. "Load frequency control of a microgrid employing a 2D Sine logistic map based chaotic sine cosine algorithm", *Appl. Soft Comput.*, **109**, 107564 (2021). https://doi.org/10.1016/j.asoc.2021.107564

24. Yousef, A.M., Ebeed, M., Abo-Elyousr, F.K., et al. "Optimization of PID controller for hybrid renewable energy system using adaptive sine cosine algorithm", *Int. J. Renew. Energy Res.*, **10**(2), pp. 669–677 (2020). https://doi.org/10.20508/ijrer.v10i2.10685.g7938

25. Khadanga, R.K., Kumar, A., and Panda, S. "A novel sine augmented scaled sine cosine algorithm for frequency control issues of a hybrid distributed two-area power system", *Neural Comput. Appl.*, **33**, pp. 12791–12804 (2021). https://doi.org/10.1007/s00521-021-05923-w

26. Debbarma, S., Saikia, L.C., and Sinha, N. "Automatic generation control using two degree of freedom fractional order PID controller", *Int. J. Electr. Power Energy Syst.*, **58**, pp. 120–129 (2014). https://doi.org/10.1016/j.ijepes.2014.01.011

27. Mirjalili, S.M., Mirjalili, S.Z., Saremi, S., et al., *Sine Cosine Algorithm: Theory, Literature Review, and Application in Designing Bend Photonic Crystal Waveguides*, Springer International Publishing (2020). https://doi.org/10.1007/978-3-030-12127-3_12

28. Mirjalili, S. "SCA: A Sine Cosine algorithm for solving optimization problems", *Knowledge-Based Systems*, **96**, pp. 120–133 (2016). https://doi.org/10.1016/j.knosys.2015.12.022

Biographies

Neelesh Kumar Gupta born in 1991. He received B. Tech degree form UPTU Lucknow, Utter Pradesh, India in electrical and electronics engineering in 2014, M. Tech in Power System Engineering from NIT Jamshedpur, Jharkhand, India, in 2018. Currently he is the Research Scholar in Electrical Engineering department of NIT Jamshedpur Jharkhand, India.

Manoj Kumar Kar born in 1988. He received B. Tech degree from B.P.U.T, Odisha India, in 2010, M. Tech (Power Electronics and Control Drives) from VSSUT, Burla, Odisha, India, in 2012. He is having five years of teaching experience. Currently, he is the Research Scholar in the Electrical Engineering Department, NIT Jamshedpur Jharkhand, India.

Arun Kumar Singh born in 1956. He received his BSc (Engg.) degree from Kurkshetra University, India in 1982, M Tech from IIT BHU, India in 1985, PhD from IIT Kharagpr, India in 1994. He is having more than thirty years of teaching experience. Currently, he is working as Professor in the Electrical Engineering Department, NIT Jamshedpur Jharkhand, India.